Analytical Methods

Accepted Manuscript

This article can be cited before page numbers have been issued, to do this please use: X. Wu, W. li, G. Zhang, Q. Zhang and Y. Cheng, *Anal. Methods*, 2014, DOI: 10.1039/C4AY01498G.

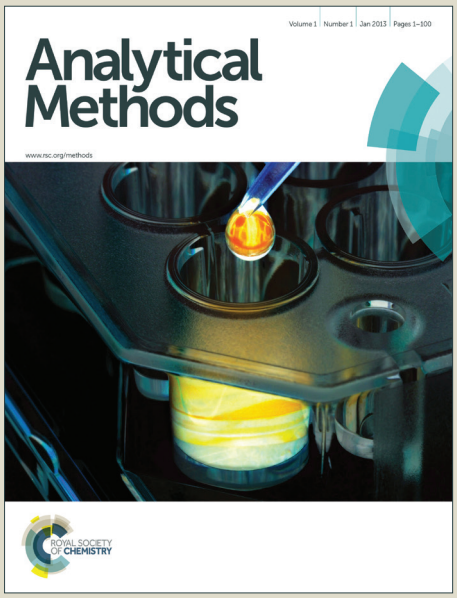

ROYAL SOCIETY OF CHEMISTRY

www.rsc.org/methods

View Article Online
DOI: 10.1039/C4AY01498G

High sensitive glucose biosensor preliminary applied for detecting of glucose levels of cerebrospinal fluid in patients with traumatic brain injury

Xiaohui Wu[a], Wenjuan Li[b], Guangliang Zhang[c], Qingtao Zhang[d], Yuan Cheng[a*]

a Department of Neurosurgery, The Second Affiliated Hospital of Chongqing Medical University, Chongqing, 400010, China

b Institute of Life Sciences, Chongqing Medical University, Chongqing, 400016, China

c Department of Neurosurgery, Jiangjin Centre Hospital, Chongqing, 402260, China

d Department of Neurosurgery, Chongqing The Fourth Hospital, Chongqing, 400014, China

Abstract

Traumatic brain injury (TBI) has been associated with an acute stress response mediated by the sympathoadrenomedullary axis, which can be assessed by measuring glucose level. Thus, aiming for a more convenient assay system of glucose, a novel electrochemical measurement for sensitive detection of glucose in cerebrospinal fluid (CSF) was developed in this work in virtue of electrodeposition of platinum nanoclusters on the stable composite films of carbon nanotubes (CNTs) and core-shell

* Corresponding author. **Fax:** +862363822815. **E-mail addresses:** yuancheng811211@163.com (Y.Cheng).

View Article Online
DOI: 10.1039/C4AY01498G

organosilica@chitosan nanospheres (OrgSi@CS) modified glassy carbon electrode. The morphologies and the structures of the OrgSi@CS-CNTs composite material and platinum nanoclusters were characterized by atomic force microscopy (AFM), transmission electron microscopy (TEM) and X-ray photoelectron spectroscopy (XPS). Cyclic voltammetries (CVs) were used to feature the direct electrochemistry behavior between the electroactive center of glucose oxidase (GOD) and electrode. The linear response range was determined from 1.2×10^{-6} to 1.6×10^{-3} M with a detection limit of 4.0×10^{-7} M, and the Michaelies-Menten constant (K_M^{app}) value was estimated to be 0.41 mM, indicating a high-catalytic activity of glucose. *In vitro* experiments were performed with clinical samples of CSF obtained from TBI patients and compared with the glucose oxidase endpoint method, which showed an accepted measurement with enhanced rapid and convenient, indicating the feasibility of the sensors for a real-time continuous monitoring *in vivo*.

Keywords： Carbon nanotubes; Platinum nanoclusters; Core-shell organosilica@chitosan nanospheres; Traumatic brain injury; Cerebrospinal fluid.

1. Introduction

Traumatic brain injury (TBI) is a major cause of death and disability among a predominantly young population [1]. The metabolic characteristics of severe TBI are glucose demand increase, brain glucose metabolism disturbed and energy failure [2,3]. Episodes of hyperglycemia as well as hypoglycemia are considered to be secondary insults in patients with TBI [4]. Generally, hyperglycemia, defined as blood glucose levels ranging from 10 to 16.6 mmol/L, aggravates underlying brain damage and

View Article Online
DOI: 10.1039/C4AY01498G

influences both morbidity and mortality in head-injured patients [5, 6] by inducing tissue acidosis [7], oxidative stress, and cellular immunosuppression [8] as well as following multitrauma [9]. On the other hand, hypoglycemia impairs energy supply causing metabolic perturbation [10] and inducing cortical spreading depolarizations [11]. Thus, monitoring of glucose levels in cerebrospinal fluid (CSF) should be of great value and help to avoid episodes of hypo- or hyperglycemia. Currently, in many neurointensive care units, microdialysis and glucose oxidase endpoint method (GLU-GOD-PAP) have been widely used to monitor glucose metabolism after acute brain injury [12]. The microdialysis technique can not reflect the real metabolism level of blood glucose in the whole intracranial environment, only monitor the local cerebral damage, and little is known about the correlation of brain glucose values obtained by microdialysis. The GLU-GOD-PAP method usually was used to support from the kits, which need the high cost. Thus, the accurate and convenient analysis of the CSF glucose in brain injury patients has been challenged. Recently, the analytical techniques of some small biological molecules, such as glucose, etc, have been widely reported and well used in the research field of life sciences and clinical medicine [13-15]. Thereinto, electrochemistrical biosensor, has received tremendous attention to detect glucose due to its high sensitivity and selectivity [16-18]. In this study, we assessed the glucose level in CSF by virtue of electrochemistrical biosensor method. As far as we know, similar works were seldom reported.

In the manufacturing process of a biosensor, carbon nanotubes (CNTs) with their exceptional structures and electronic properties, such as ballistic transport over length scales of several hundred nanometers, are very promising for potential applications in

View Article Online
DOI: 10.1039/C4AY01498G

chemical sensors and biosensors [19]. Recently, composite materials based on integration of CNTs and some other materials have received increasing interest because of their properties of the individual components with a synergistic effect on the performance of biosensors. Materials for such purposes include conducting polymers, redox mediators and metal nanoparticles [20-22], and so on.

Recently, inorganic-organic core-shell nanospheres have attracted a great deal of attention because they display superior physicochemical properties to their single component counterparts as well as additional novel properties [23-25]. So such kind of nanomaterials have been shown to be promising for various energy applications in cosmetics, paints, optics and electronics [26,27]. In this study, we have employed a facile and bottom-up method to synthesize organosilica@chitosan (OrgSi@CS) nanospheres basing on synergic grafting polymerization, sol–gel reaction and amphiphilic self-assembly technologies. The resulted OrgSi@CS consisted of organosilica as core and chitosan containing rich -NH_2 groups as shell [28]. Moreover, the OrgSi@CS, with large surface area and high-surface free energy, displayed a highly positive ζ-potential value +68 mV, excellent film-forming ability and a favorable microenvironment for immobilizing negatively charged enzymes [29].

As we known, the direct electron transfer (DET) between biomolecules is of fundamental importance in life science and design of bioelectronics devices, biosensors systems [30-32]. However, the redox-active center of enzyme is deeply embedded within an insulative protein shell, which results in the extremely difficult of DET between the electrode and the enzyme [33]. So using nanoparticles to enzyme-based system has recently been proposed to overcome this problem by employing nanoparticles to provide

View Article Online
DOI: 10.1039/C4AY01498G

an efficient electron relay pathway [34,35]. In most of the reported literatures, large-size nanoparticles have been used to immobilize protein as an extension of the electrode surface, which made proteins with poor orientation or inappropriate alignment of the redox center and resulted in inefficient DET to electrode surfaces. With this consideration, suitable size nanoparticles for integration into the protein must be employed. Nanoclusters, with small particle size (1-10 nm) and narrow size distribution, were distinct from traditional colloids as a new type of nanomaterial. Accordingly, a recent book reviews metal nanoclusters states, that is "Metal nanoparticles are certain to be the building blocks of the next generation of electronic, optoelectronic, and chemical sensing devices" [36,37]. In present work, we prepared poly(N-vinyl-2-pyrrolidone) (PVP) protected Pt nanoclusters (called "Pt NCs" for short) with a high metal/PVP ratio aiming to prevent the small metal nanoclusters from aggregating in water or in ethanol. The Pt NCs (about 2.5 nm) are much smaller than the enzyme molecule (about 7 nm), and can act as good electrical conductors between the electrode and GOD.

Considering the advantage of the CNTs, OrgSi@CS and Pt NCs, we have integrated them in a biosensor fabrication to exploit their synergistic augmentation on the improvement of sensor characteristics. The DET of between GOD and glassy carbon electrode (GCE) was realized in the proposed biosensor and displayed high electroactivity and electorcatalytic response to glucose. The electrochemical performances of the developed electrodes were studied in details and used to assess the glucose level in CSF.

2. Experimental

2.1. Chemicals

View Article Online
DOI: 10.1039/C4AY01498G

CNTs (>95% purity) were obtained from Chengdu Organic Chemicals Co. Ltd. of the Chinese Academy of Science and purified by fluxing in concentrated nitric acid for 7 h prior to use. Glucose oxidase (GOD), chitosan (CS, from crab shells, Mw: 100,000–300,000, deacetylating grade: 70-85%), 3-(trimethoxysilyl) propyl methacrylate (TMSPM), *tert*-butyl hydroperoxide (TBHP, 70% solution in water), Poly(N-vinyl-2-pyrrolidone) (PVP, average molecule weight 50000) and glucose were all purchased from Sigma, and used as received. Hydrogen hexachloroplatinate (IV) hexahydrate ($H_2PtCl_6 \cdot 6H_2O$, 99%), acetic acid and hydrogen peroxide (30% solution) were gained from Chemical Reagent Co., Chongqing, China. Phosphate buffered saline (PBS) solutions with different pH values were prepared with stock standard solutions of 0.1 M KH_2PO_4 and 0.1 M Na_2HPO_4. The supporting electrolyte was 0.1 M KCl. GOD stock solutions (2 mg/mL) were prepared with 0.1 M pH 6.0 PBS. The PVP-protected Pt NCs (called "Pt NCs" for short) with mean size of 2.5 nm were prepared for using the "unprotected" Pt nanoclusters as building blocks according to the literature [38]. Cerebrospinal fluid that was drained from TBI patients in the course of their treatment was obtained from the Fourth People's Hospital of Chongqing, China.

2.2. Apparatus and measurements

Amperometric experiments and cyclic voltammetric experiments were performed on a CHI 660A electrochemical work station (Shanghai CH Instruments Co., China) with a conventional three electrode systems consisted of a modified glassy carbon electrode (GCE) as working electrode, a platinum wire as auxiliary electrode, and a saturated calomel electrode (SCE) as reference electrode. All potentials were measured and reported versus the SCE. All the electrochemical experiments were carried out at room

View Article Online
DOI: 10.1039/C4AY01498G

temperature. Transmission electron microscopy (TEM) was carried out on a TECNAI 10 (PHILIPS FEI Co., Holland). The atomic force microscopy (AFM) images were obtained as a scanning probe microscope (SPA 400, Japan).

2.3. Preparation of the modified electrode

An OrgSi@CS-CNTs composite (1.0 mg/mL) was achieved according to reference [28] as follows: (i) 100 mL 0.5 wt% chitosan solution containing 0.6 wt% acetic acid was purged with nitrogen for 30 min under stirring in a flask, after that, about 2 mL TMSPM monomer was added at 80 ^{o}C. Then 1 mL 20 mM TBHP aqueous solution was added immediately, and the mixture was stirred for 4 h under nitrogen. Finally, stable latex was obtained, which was carefully centrifugation, decantation and resuspending in 0.6 wt% acetic acid solutions. (ii) 3 mg of the acid-treated CNTs were dispersed into 3 mL of OrgSi@CS-CNTs nanospheres suspension by stirring constantly.

A GCE (4 mm diameter) was carefully polished using 0.3 and 0.05 μm alumina slurry, respectively, then ultrasonically cleaned in ethanol and water successively and was allowed to dry at room temperature. Subsequently, 8 μL of OrgSi@CS-CNTs suspension was cast onto a pretreated GCE surface. After solvent water was evaporated, an OrgSi@CS-CNTs/GCE was obtained. And then Pt NCs were electrodeposited on the OrgSi@CS-CNTs films by the potential step deposition method for accumulation of Pt NCs for 3 min at -0.25 V. Finally, the resulting electrode was immersed in a 2 mg/mL GOD solution for 10 h to attach enzyme molecules to the electrode surface, which was denoted here as GOD/Pt NCs/OrgSi@CS-CNTs/GCE. The resulting biosensor was stored in a refrigerator (4 °C) for further use. The preparation process of the biosensor was shown in Scheme 1.

View Article Online
DOI: 10.1039/C4AY01498G

Scheme 1

3. Results and discussion

3.1 Characterization of Pt NCs

The preparation of a homogeneous solution of Pt NCs was a key step in this work process. To confirm the structure of Pt NCs, typical TEM was performed in Fig. 1.

Fig. 1

The result has revealed that the Pt NCs were highly dispersed spherical particles with a mean diameter of 2.5 nm and no aggregation occurs during store process for several months at 4 °C.

3.2 AFM and XPS analysis

In order to investigate the surface topographies of different films, AFM analysis was performed at OrgSi@CS, OrgSi@CS-CNTs, and GOD/Pt NCs/OrgSi@CS-CNTs composite films in Fig. 2.

Fig. 2

As shown in Fig. 2A, the AFM micrograph of OrgSi@CS film presents clearly globous structures and the size was distributed in 40-80 nm with mean sizes around 60 nm, which covering the entire surface of the substrate. When CNTs were dispersed into OrgSi@CS nanospheres suspension, the AFM image of the resulting composites (Fig. 2B) displayed overlaying abundantly CNTs with OrgSi@CS. In the case of GOD/Pt NCs/OrgSi@CS-CNTs film (Fig. 2C), the surface morphology became blurry, which might be ascribed to GOD molecules filling the interstitial place. The XPS measurement will further confirm the existence of Pt NCs since XPS could examine the chemical composition and the valence states of elements. Fig. 2D illustrated that the XPS spectra

View Article Online
DOI: 10.1039/C4AY01498G

of OrgSi@CS-CNTs (a) and Pt NCs/OrgSi@CS-CNTs (b) composites. As shown in Fig. 2D (a), there were the characteristic of intense O1s signal, C1s signal, N1s signal, Si2p signals, which should attribute to the respective atoms in OrgSi@CS-CNTs. When Pt NCs were loaded onto the OrgSi@CS-CNTs composites, as expected, the Pt 4f region exhibited doublets from the spin-orbit splitting of 70.9 eV for $4f_{7/2}$ and 74.7 eV $4f_{5/2}$ states (see the inset of Fig. 2D (b)). The peak of Pt $4f_{7/2}$ can be used to affirm the presence of metallic platinum Pt(0), and the Pt $4f_{5/2}$ peak was attributed to the presence of oxidation states of Pt, which indicated that Pt NCs were attached to the electrode surface.

3.3 Electrochemical characteristics of the modified electrode

Fig. 3 showed the cyclic voltammograms (CVs) of the modified electrode in each assembly step in 0.1 M PBS (pH 6.0).

Fig. 3

There was no obvious redox peaks were observed after the formation of Pt NCs/OrgSi@CS-CNTs (curve a in Fig. 3) composite membranes on bare GCE in the potential range of −0.7 to -0.15 V. When GOD was immobilized into the OrgSi@CS-CNTs film matrix, a pair of well-defined redox peaks was appeared (curve b in Fig. 3), the redox peaks were located at -0.39 and -0.44 V, respectively. The separation of peak potentials (ΔE_p) is ca. 50 mV and the ratio of cathodic and anodic peak currents were about unity. The formal potential ($E^{0'}$) calculated was estimated as ca. -0.42 V, which is close to the reported literatures [39]. It can be concluded that the redox waves should be ascribed only to GOD, and all of these electrochemical parameters indicate that the reaction of GOD undergoing at the modified electrode is a quasi-reversible redox process. After Pt NCs were immobilized on the electrode surface, a peak current increase

View Article Online
DOI: 10.1039/C4AY01498G

as shown in Fig. 3c, which might be attributed to the small–size Pt NCs could well enhanced the conductibility, more effective promote the electron transfer between redox sites of enzyme and sensing surface and more favorable orientation environment of GOD molecules.

Fig. 4 shows the CVs of the GOD/Pt NCs/OrgSi@CS-CNTs/GCE electrode at different scan rates.

Fig. 4

It was found that the anodic peak potential of the enzyme electrode shifted to a more positive value with increasing scan rate, while the cathodic peak potential shifting to a negative direction. Simultaneously, the peak current increases with increasing scan rate. As shown in Fig. 4a, in the scan rates from 50 to 500 mV/s, the redox peak currents rise linearly with the scan rate, insinuating that the electrochemical behavior of GOD has the typical property of a surface electrochemical process. Meanwhile, the linear relationships between the peak potential (E_p) and the logarithm of the scan rate (log v) for both the cathodic and anodic peaks were also plotted. The E_{pa} and E_{pc} were proportional to log v (inset b of Fig. 4). By using the model of Laviron [40], the charge transfer coefficient (α) of 0.5 was calculated by the slope of Fig. 4b, and the apparent heterogeneous electron transfer rate constant (k_s) was further calculated through the following equation and the result was obtained as ca. 4.861 s^{-1}.

$$\log k_s = \alpha \log(1-\alpha) + (1-\alpha)\log\alpha - \log\left(\frac{RT}{nFv}\right) - \alpha(1-\alpha)\frac{nF\Delta E_p}{2.3RT}$$

The catalytic activity of the biosensor toward glucose was investigated by cyclic voltammetry. Fig. 5 illustrates the CVs recorded for the biosensor in PBS (pH 6.0) containing varied concentration of glucose.

View Article Online
DOI: 10.1039/C4AY01498G

Fig. 5

With the addition of glucose, reduction peak current decreased significantly while oxidation peak current increased, indicating that a catalytic reaction occurred on this biosensor. It can be explained that glucose is the substrate of GOD, whose presence will result in an enzyme-catalyzed reaction and decrease the concentration of the oxidized form of GOD, which can be summarized as following two processes:

$$GOD(ox) + glucose \rightarrow GOD(red) + gluconolactone + 2H^+ \quad (1)$$

$$GOD(red) + 2H^+ + O_2 \rightarrow GOD(ox) + H_2O_2 \quad (2)$$

Based on the decrease of the reduction current, the concentration of glucose can be detected.

3.4. Dependence of DET of GOD on solution pH

The effect of solution pH on the response of immobilized GOD is shown in Fig. 6.

Fig. 6

With pH value increasing, both catholic and anodic peak potentials shifted to negative direction. In the inset of Fig. 6, $E^{0'}$ has a linear relationship with pH from 4.0 to 8.0 with a slope of -49.6 mV/pH, which is similar to the theoretical value of -58.5 mV/pH [39] for a reversible. That was attributed to the FAD undergo a redox reaction as follows:

$$GOD\text{-}FAD + 2e^- + 2H^+ \leftrightarrow GOD\text{-}FADH_2$$

It proves that it is a two-electron coupled with two-proton reaction, peak potentials should be pH-dependent. As shown in Fig. 5, the maximum current response is present at pH 6.0. The decrease of GOD response at high pH maybe ascribe the decrease of proton concentration, while at low pH likely attributing to the loss of bioactivity of GOD.

View Article Online
DOI: 10.1039/C4AY01498G

3.5. Response of the biosensor to glucose

Fig. 7 shows a typical current–time curve of the biosensor under the optimized experimental conditions after the addition of successive the glucose concentration to the PBS under stirring.

Fig. 7

With the addition of the concentration of substrate, the biosensor responded rapidly. The inset of Fig. 6 demonstrates the calibration curve of the biosensor for glucose determination. The response current increases linearly with the glucose concentration in the range of 1.2×10^{-6} to 1.6×10^{-3} M with a correlation coefficient of 0.998 (n = 20), and the detection limit of 4.0×10^{-7} M is estimated at signal-to-noise ration of three. When the concentration of glucose is higher than 1.6×10^{-3} M, a response plateau appears, showing that the characteristics of the Michaelis-Menten kinetic mechanism. The apparent Michaelis-Menten constant (K_M^{app}) is calculated to be 0.41 mM according to the Lineweaver-Burk equation [41].

3.6. Precision of measurements and stability of biosensor

The intra-assay precision of the biosensors was evaluated by assaying one enzyme electrode for six replicate determinations under the same conditions. Similarly, the inter-assay precision was estimated at eight different electrodes. The relative standard deviation (R.S.D.) of intra-assay and inter-assay were calculated to be 3.1% and 4.6%, indicating acceptable precision and reproducibility.

Stability is an important requirement for fabrication of glucose sensors. Usually, the stability of biosensors contains operational stability and storage stability. The storage stability of the enzyme electrode was investigated over 1 month. It was found that the

View Article Online
DOI: 10.1039/C4AY01498G

current response retained 84.1% of its original response over 30 days later, showing a longer lifetime. The operational stability of the biosensors was examined depending on continuous cyclic voltammetric scanning. When 100 continuous cyclic scans were performed in the potential range from -0.7 to -0.15 V with a 50 mV/s scan rate, just 3.3% decrease of the initial response was detected, showing well operational stability. The good stability may be due to the fact that the OrgSi@CS-CNTs matrix was stable for adsorbing biomolecules. On the other hand, the Pt NCs could decrease the electron-transfer impedance and provide an appropriate microenvironment for retaining the bioactivity of the enzyme molecules.

3.7. Interference determination

To test the anti-interferent ability of the proposal strategy for glucose detection, the possible influences of some other biocompounds such as ascorbic acid, uric acid, acetaminophen and L-cys were examined by measurement of 0.2 mM glucose in PBS containing a specified concentration of the interfering compounds (0.01 mM ascorbic acid, 0.05 mM uric acid, 0.01 mM acetaminophen and 0.5 mM L-cys) under the same experimental conditions. As shown in Table 1, all of the tested compounds have no significant effect on the current intensity compared with the absence of glucose, which shows that the above four tested substances did not interfere significantly for glucose detection.

3.8 Analysis of human cerebrospinal fluid samples in intro

Five human cerebrospinal fluid samples were analyzed to evaluate performance of the proposed glucose biosensor in clinical analysis. The accuracy of glucose determination was examined by comparing the results with those from the clinical analysis method

View Article Online
DOI: 10.1039/C4AY01498G

(GLU-GOD-PAP method). The results are listed in Table 2. The samples were diluted by ten times and the relative deviation of these results is between -6.45% and 8.69%. The results were satisfactory and agree closely with the both analytical methods, which indicated a new tool for the analysis of glucose metabolism in the CSF. Since the use of biosensor technique is simply and sensitive, it is possible to use the methodology in patient studies of glucose metabolism after brain injuries.

4. Conclusions

In this paper, we described the construction of a new, effective electrochemical biosensing platform of glucose by modifying a GCE with Pt NCs and OrgSi@CS-CNTs composite films to detect the glucose of cerebrospinal fluid samples. The method is advantageous in terms of its simplicity, sensitively and rapidly in operation and instrumentation compared with the existing methods for the detection of glucose in cerebrospinal fluid. However, this method was only studied for *in vitro* detection and the equipment had not achieved the miniaturization and integration. This work is a new attempt to detect brain glucose *in vitro* by the method of biosensor. Furthermore, the next step will be to conduct a trial of the smart microsensors *in vivo* using an animal model to further broaded biosensor's application.

Acknowledgements

This work was supported by the National Natural Science Foundation of China (No. 30870723, 21205146).

References

[1] Q. J. Zhao, X.G. Zhang, L.X. Wang, Journal of Critical Care, 2011, 26, 311-315.

[2] V.P. Bergsneider M, N. Hattori, H.M. Wu, S.C. Huang, N.A. Martin, T.C. Glenn, D.L.

View Article Online
DOI: 10.1039/C4AY01498G

McArthur, D.A. Hovda, J Cereb Blood Flow Metab, 2005, 125, 763-774.

[3] R.L. Hayes, Y. Katayama, L.W. Jenkins, B.G. Lyeth, G.L. Clifton, J. Gunter, J.T. Povlishock, H.F. Young, J Neurotrauma, 1988, 5, 121-137.

[4] J. Kreutziger, V. Wenzel, A. Kurz, M.A. Constantinescu, Intensive Care Med, 2009, 35, 1234-1239.

[5] P. Diaz-Parejo, N. Stahl, W. Xu, P. Reinstrup, U. Ungerstedt, Intensive Care Med 2003, 29, 544-550.

[6] E. Jeremitsky, L.A. Omert, C.M. Dunham, J. Wilberger, A. Rodriguez, J Trauma, 2005, 58, 47-50.

[7] D.A. Zygun, L.A. Steiner, A.J. Johnston, P.J. Hutchinson, P.G. Al-Rawi, D .Chatfield, P.J. Kirkpatrick, D.K. Menon, A.K. Gupta, Neurosurgery, 2004, 55, 877-881.

[8] D. Aronson, Adv Cardiol, 2008, 45, 1-16.

[9] J.L. Sperry, H.L. Frankel, S.L. Vanek, A.B. Nathens, E.E. Moore, R.V. Maier, J.P. Minei, J Trauma, 2007, 63, 487-493.

[10] P. Vespa, R. Boonyaputthikul, D.L. McArthur, C. Miller, M. Etchepare, M .Bergsneider, T. Glenn, N. Martin, D. Hovda, Crit Care Med, 2006, 34, 850-856.

[11] A.J. Strong, J.A. Hartings, J.P. Dreier, Curr Opin Crit Care, 2007, 13, 126-133.

[12] E. Rostami, B.M. Bellander, Journal of Diabetes Science and Technology, 2011, 5, 596-604.

[13] C.X. He, J.H. Liu, Q.L. Zhang, C. Wu, Sensors and Actuators B, 2012, 166, 802-808.

[14] J.J. Yu, D.L. Yu, T. Zhao, B.Z. Zeng, Talanta, 2008, 74, 1586-1591.

[15] K.Y. Hwa, B. Subramani, Biosensors and Bioelectronics, 2014, 62, 127-133.

View Article Online
DOI: 10.1039/C4AY01498G

[16] M.D. Rubianes, G.A. Rivas, Analytica Chimica Acta, 2001, 440, 99-108.

[17] Z.F. Sun, D. Liu, H. Gan, R.J. Shen, M.H. Yang, Y. Zhang, Biosensors and Bioelectronics, 2013, 39, 215-219.

[18] Y. Takahashi, A. Shevchuk, P. Novak, Y. Murakami, H. Shiku, Y. Korchev, T. Matsue, Journal of the American Chemical Society, 2010, 132, 10118-10126.

[19] M.S. Dresselhaus, G. Dresselhaus, P. Avouris, Springer-Verlag: New York, 2001, 213-247.

[20] M. Zhang, W. Gorski, Journal of the American Chemical Society, 2005, 127, 2058-2059.

[21] Y.J. Zou, L.X. Sun, F. Xu, Biosensors and Bioelectronics, 2007, 22, 2669-2674.

[22] A.I. Gopalan, K.P. Lee, D. Ragupathy, S.H. Lee, J.W. Lee, Biomaterials, 2009, 30, 5999-6005.

[23] J. Kim, J.E. Lee, J. Lee, Y. Jang, S.W. Kim, K. An, J.H. Yu, T. Hyeon, Angewandte Chemie International Edition, 2006, 45, 4789-4783.

[24] S.I. Stoeva, F. Huo, J.S. Lee, C.A. Mirkin, Journal of the American Chemical Society, 2005, 127, 15362-15363.

[25] K.S. Soppimath, L.H. Liu, W.Y. Seow, S.Q. Liu, R. Powell, P. Chan, Y.Y. Yang, Advanced Functional Materials, 2007, 17, 355-362.

[26] F. Caruso, Weinheim: Wiley-VCH, 2004.

[27] M.H. Yang, Y.H. Yang, Y.L. Liu, G.L. Shen, R.Q. Yu, Biosensors and Bioelectronics, 2006, 21, 1125-1131.

[28] B. Fei, H.F. Lu, J.H. Xin, Polymer. 2006, 47, 947-950.

[29] S.H. Chen, R. Yuan, Y.Q. Chai, B. Yin, W.J. Li, L.G .Min, Electrochimica Acta,

View Article Online
DOI: 10.1039/C4AY01498G

2009, 54, 3039-3046.

[30] C. Fan, K.W. Plaxco, A.J. Heeger, Journal of the American Chemical Society, 2002, 124, 5642-5643.

[31] Y. Tian, L. Mao, T. Okajima, T. Ohsaka, Analytical Chemistry, 2002, 74, 2428-2434.

[32] X. Wei, J. Cruz, W. Gorski, Analytical Chemistry, 2002, 74, 2428-2434.

[33] H. Y. Gu, A. M. Yu, and H. Y. Chen, J. Electroanal. Chem., 2001, 516, 119.

[34] J.M. Abad, M. Gass, A. Bleloch, D.J. Schiffrin, Journal of the American Chemical Society, 2009, 131, 10229-10236.

[35] E. Katz, I. Willner, Chem. Phys. Chem. 2004, 5, 1084-1140.

[36] R. Ferrando, J. Jellinek, R.L. Johnston, Chemical Reviews, 2008, 108, 845-910.

[37] D.L. Feldheim, C.A. Foss Jr, Marcel Dekker: New York, 2002, 207-236.

[38] Y. Wang, J.W. Ren, K. Deng, L.L. Gui, Y.Q. Tang, Chemistry of Materials, 2000, 12, 1622-1627.

[39] S.Q. Liu, H.X. Ju, Biosensors and Bioelectronics, 2003, 19, 177-183.

[40] E. Laviron, Journal of Electroanalytical Chemistry, 1979, 101, 19-28.

[41] R.A. Kamin, G.S. Wilson, Analytical Chemistry, 1980, 52, 1198-1205.

View Article Online
DOI: 10.1039/C4AY01498G

Figure caption

Scheme 1. Illustration of the preparation process of modified electrode.

Fig. 1. TEM image of Pt NCs.

Fig. 2. AFM images of OrgSi@CS membrane (A), OrgSi@CS-CNTs composite membrane (B), and GOD/Pt NCs/OrgSi@CS-CNTs (C), and the XPS spectra of OrgSi@CS-CNTs (a) and Pt NCs/OrgSi@CS-CNTs (b) composite films (D). Inset: Pt 4f XPS spectra of Pt NCs/OrgSi@CS-CNTs.

Fig. 3. CVs of the OrgSi@CS-CNTs/GCE (a), GOD/OrgSi@CS-CNTs/GCE (b), GOD/Pt NCs/OrgSi@CS-CNTs/GCE (c) in 0.1 M pH 6.0 PBS at scan rate of 50 mV/s.

Fig. 4. CVs of GOD/Pt NCs/OrgSi@CS-CNTs/GCE electrode in 0.1 M PBS (pH 6.0) at different scan rates (from inner to outer): 50, 100, 200, 300, 400 and 500 mV/s. Inset (a): the plots of peak currents *vs* scan rate; Inset (b): the plots of anodic and cathodic peak potential *vs.* logarithm of scan rate.

Fig. 5. CVs of the GOD/Pt NCs/OrgSi@CS-CNTs/GCE in the PBS containing 0, 0.6, and 1.2 mM of glucose (curve a and c, from bottom to top).

Fig. 6. CVs of GOD/Pt NCs/OrgSi@CS-CNTs/GCE electrode in 0.1 M PBS (pH 6.0) at various pH values (from right to left): (a) 4.0, (b) 5.0, (c) 6.0, (d) 7.0 and (e) 8.0 at a scan rate of 50 mV/s. The inset: the plot of formal potential *vs* pHs.

Fig. 7. Amperometric response of the biosensor to glucose in a pH 6.0 PBS upon successive additions of glucose. Inset shows linear calibration curves.

View Article Online
DOI: 10.1039/C4AY01498G

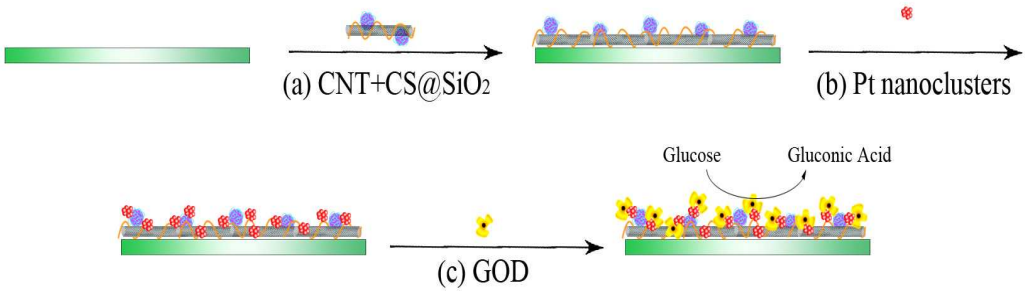

Scheme 1.

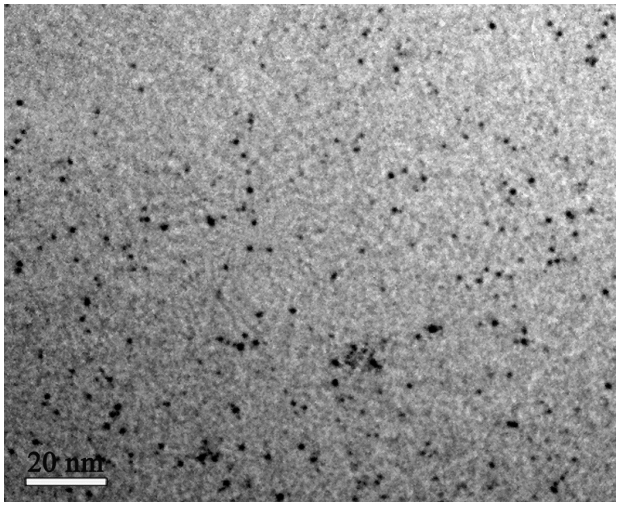

Fig. 1.

View Article Online
DOI: 10.1039/C4AY01498G

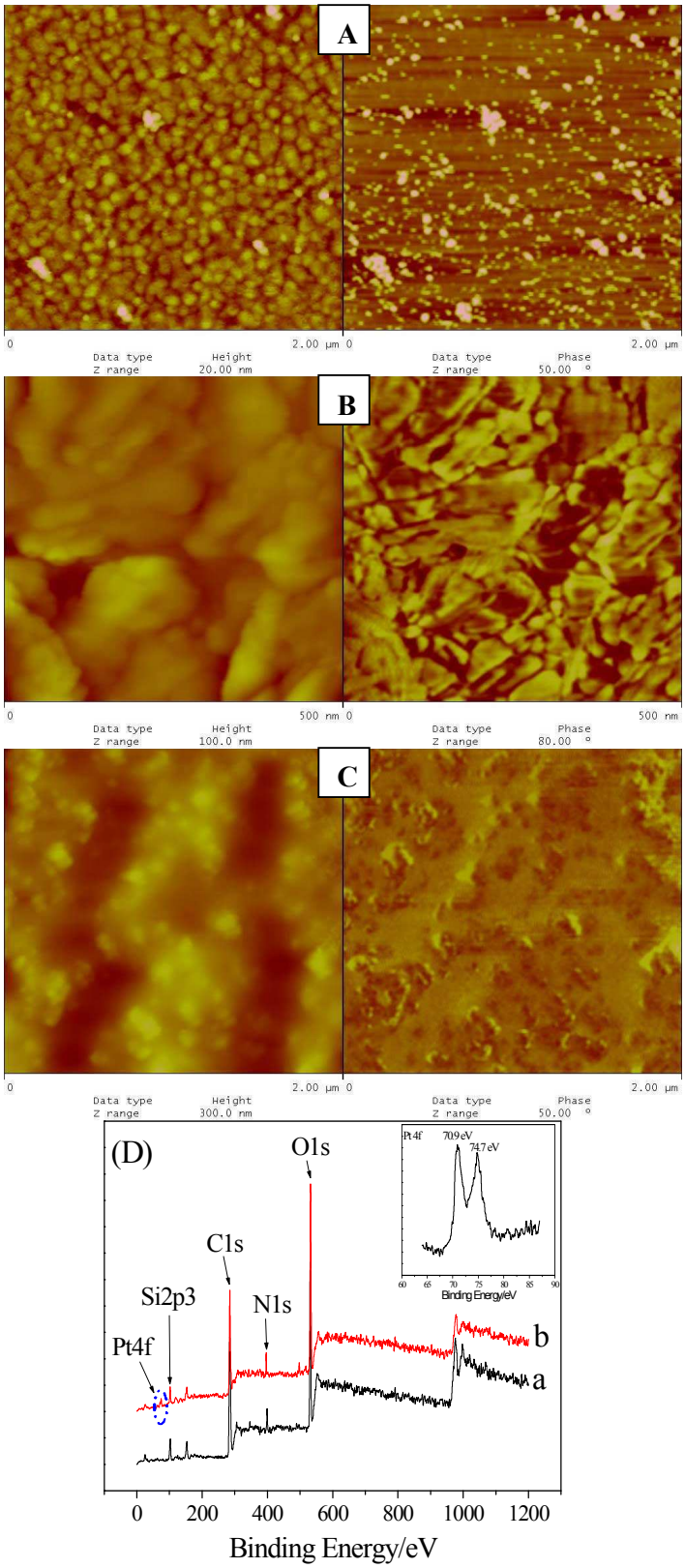

Fig. 2.

View Article Online
DOI: 10.1039/C4AY01498G

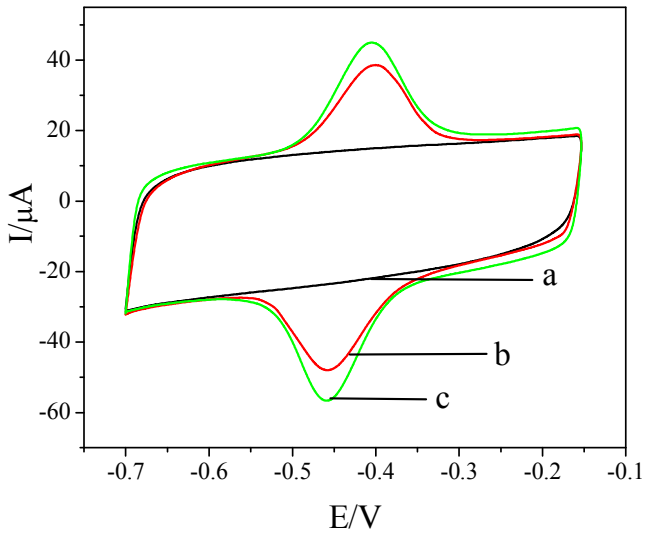

Fig. 3.

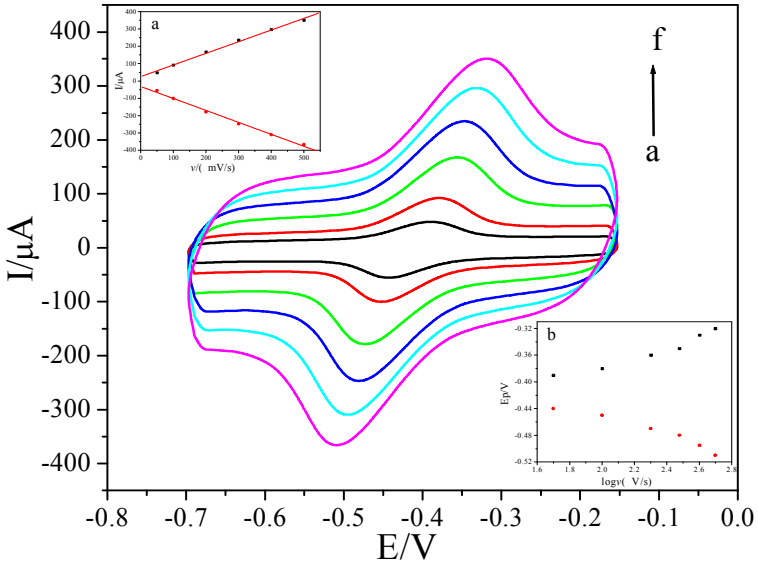

Fig. 4.

View Article Online
DOI: 10.1039/C4AY01498G

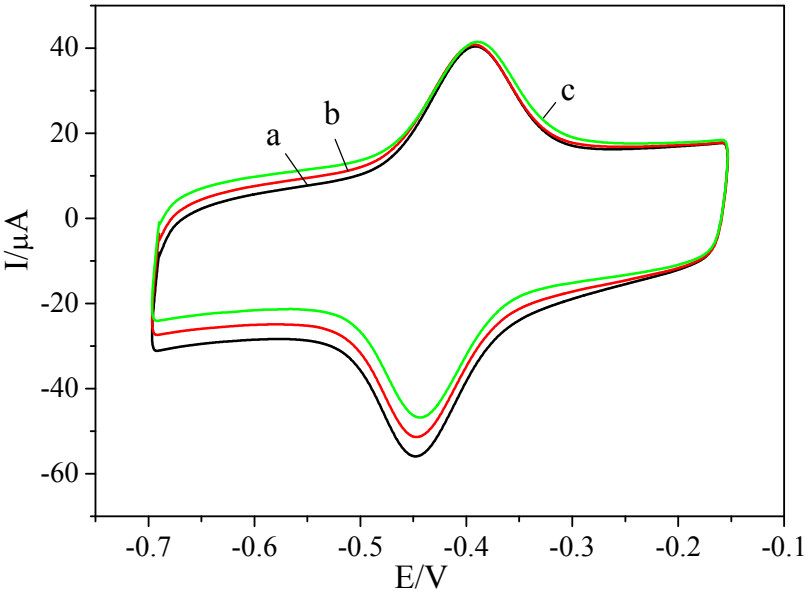

Fig. 5.

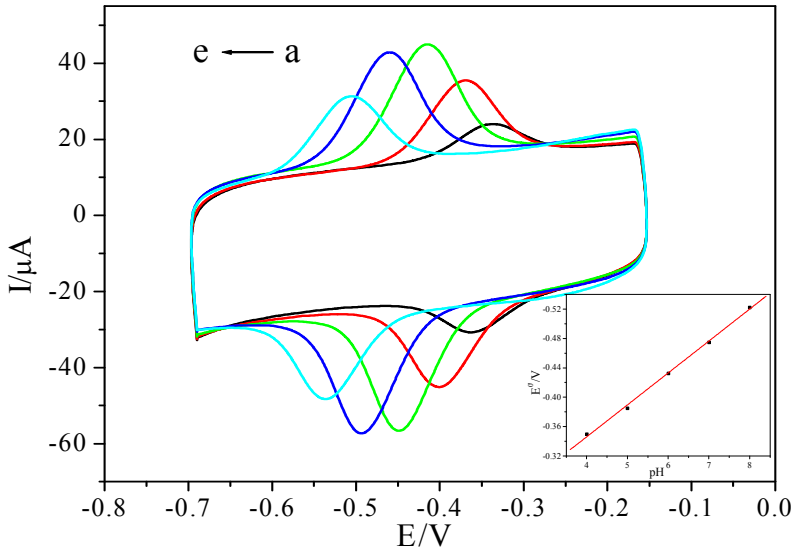

Fig. 6.

View Article Online
DOI: 10.1039/C4AY01498G

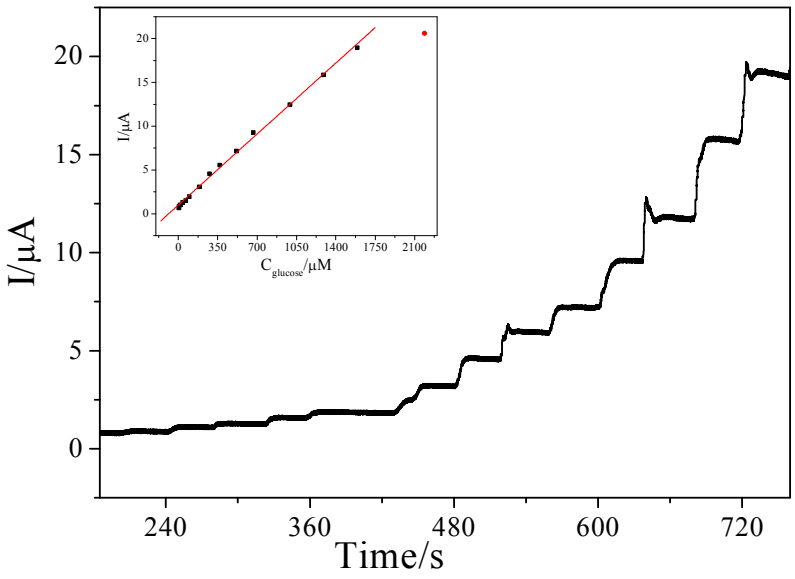

Fig. 7.

View Article Online
DOI: 10.1039/C4AY01498G

Table 1. Possible interference tested with the obtained biosensor.

Potential interfering substance	Current ratio[a] (%)
Ascorbic acid	97.6±2.3
uric acid	102.3±0.5
Acetaminophen	103.8±1.4
L-cys	98.1±2.1

[a] Mean±SD of three measurements.

View Article Online
DOI: 10.1039/C4AY01498G

Table 2. Experimental results comparison of two methods obtained in human cerebrospinal fluid samples.

Sample number	Clinical detection (mM)	From the fabricated glucose biosensor (mM)	Relative deviation (%)
1	0.35	0.33±0.02	-5.71
2	0.5	0.52±0.03	4.0
3	0.64	0.61±0.05	-4.69
4	0.31	0.29±0.01	-6.45
5	0.46	0.5±0.02	8.69